Corrosion Inhibition Effect of Substituted Thiadiazoles on Brass

X. Joseph Raj and N. Rajendran[*]

Department of Chemistry, Anna University, Chennai -600 025
[*]E-mail: nrajendran@annauniv.edu

The corrosion inhibition of thiadiazole derivatives for brass in natural seawater has been evaluated by potentiodynamic polarisation and electrochemical impedance spectroscopic techniques. It was found that the inhibition efficiency of the thiadiazole derivatives, namely, 2-amino-5-ethyl-1,3,4-thiadiazole(AETD), 2-amino-5-ethylthio-1,3,4-thiadiazole(AETTD) and 2-amino-5-tert-butyl-1,3,4-thiadiazole (ATBTD) increases with increase in concentration. The adsorption of thiadiazole derivatives on brass surface exposed to inhibitor-containing solutions was confirmed using SEM/EDX spectra and FT-IR spectra. Adsorption of these inhibitors on brass surface followed Langmuir adsorption isotherm. ICP-AES analysis confirms that dezincification was minimized to a greater extent in the presence of these inhibitors.

Keywords: Brass, SEM, Polarisation, EIS, Corrosion inhibition, Adsorption

1. INTRODUCTION

Copper and copper based alloys are of considerable importance as they form the backbone of modern industries. Brass has been widely used for shipboard condensers, power plant condensers and petrochemical heat exchangers [1, 2]. It is particularly relevant to the Indian region where various industries extensively use brass in marine applications and in heat exchanger tubes, for example, in desalination, cooling water systems and power generation. Brass materials are relatively noble and for many applications have superior physical and mechanical properties, although it could present particular corrosion problems such as dezincification and pitting corrosion in chloride-containing solutions leading to structural failure [3, 4].

When brass undergoes corrosion, a zinc oxide layer is initially formed which passivates the brass surface. When brass is dipped in a media containing chloride ion, an insoluble film of cuprous chloride is adsorbed on the brass surface. The copper ions can pass into the solution by

disproportionation reaction or it can dissolve with the formation of complexes with $CuCl_2^-$ [5, 6]. The formation of stable Cu_2O is possible inside the pores of CuCl layer. As a result the brass surface becomes enriched with copper while being impoverished by zinc during corrosion [7]. These changes make brass surface less resistant to corrosion than copper in chloride containing media [8]. Since, brass is not completely resistant to corrosion, especially in oxygen-containing electrolytes, substantial improvement in its passivity can be achieved using corrosion inhibitors. Most of the well known corrosion inhibitors are organic compounds containing polar groups having nitrogen, sulfur and/or oxygen atoms and heterocyclic compounds with polar functional groups and conjugated double bonds [9-11]. Organic heterocyclic compounds may act as inhibitors for corrosion of brass due to chelating action of heterocyclic molecules and the formation of a physical barrier on the brass surface by several mechanisms [12, 13]. The effectiveness of any corrosion inhibitor is dependent on the type of metal, properties of the corrosive environment as well as the state of inhibitor molecule.

The present work focuses on the behaviour of thiadiazole derivatives as corrosion inhibitors for 65-35 brass in natural seawater. In order to study the correlation between the molecular structure of the thiadiazole derivatives and their inhibition efficiency, electrochemical studies such as potentiodynamic polarisation and impedance spectroscopy were carried out. The characterization of the passive film was studied using FT-IR spectroscopy. The surface analysis was carried out using Scanning Electron Microscope (SEM) and the composition of brass surface was analyzed using energy dispersive X-ray analysis (EDX). The adsorption behaviour of the thiadiazole derivatives were analysed against Langmuir Adsorption isotherm theory. The concentration of the dissolved copper and zinc in the electrolyte was determined using Inductively Coupled Plasma Atomic Emission Spectroscopy (ICP-AES).
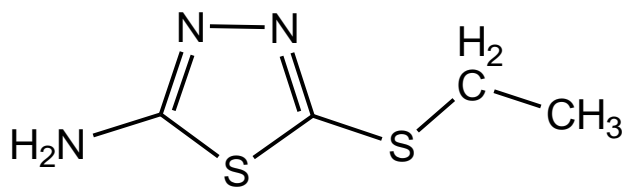
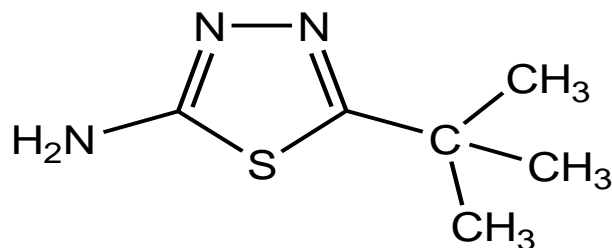## 2. EXPERIMENTAL SECTION

2.1. Materials

AETD, AETTD and ATBTD (Sigma-Aldrich, 98%) and absolute ethanol (C_2H_5OH, Fischer, 99.9 %) were used as received. The structures of thiadiazole derivatives are shown in Fig. 1.
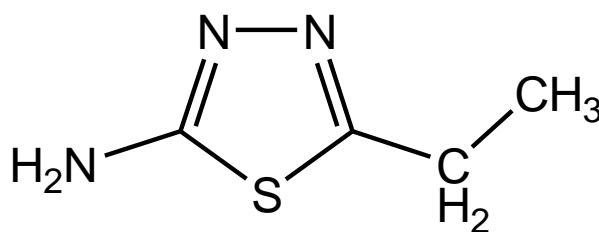
(A)

(B)

(C)

Figure 1. Chemical structure of investigated of organic inhibitors (A) 2-Amino-5-ethyl-1, 3, 4 thiadiazole (AETD) (B) 2-Amino-5-ethylthio-1, 3, 4-thiadiazol (AETTD) (C) 2-Amino-5-(4 tert-butyl)-1, 3, 4-thiadiazole (ATBTD)

The electrolyte used was the natural seawater collected in a sterilized brown flask at Eliot beach on the southern coast of Chennai, India. The working electrode used for the study having the chemical composition as wt (%) 65.3 Cu, 34.44 Zn, 0.1385 Fe, and 0.0635 Sn. The brass specimens were abraded mechanically with different grades of silicon carbide papers (400 - 1200) and washed with double distilled water. Further the samples were degreased with acetone using ultrasonicator and thoroughly washed with double distilled water and dried in air. Different concentrations of the inhibitors were added into the electrolyte to find out the optimum concentration of the inhibitor.

2.2. Potentiodynamic polarisation studies

An electrochemical cell with a three electrode assembly was used to study the electrochemical measurements. Brass specimens with exposed area of 0.28 cm^2, a platinum foil of 1 cm^2 area and silver- silver chloride Ag/AgCl in saturated KCl (Advance-Tech Controls Pvt. Ltd, India) were used as working, counter and reference electrodes respectively. The polarisation experiments were carried out using the Potentiostat/Galvanostat (Model PGSTAT 12, AUTOLAB, the Netherlands B.V) controlled by a personal computer with dedicated software (GPES version 4.9.005). The working electrode was immersed in natural seawater in the presence and absence of different concentrations of the inhibitors to which a current of -1.0 mA cm^{-2} was applied for 15 min to reduce oxides and then allowed to stabilize for 30 min. The polarisation experiments were carried out for brass specimen at a scan rate of

1 mV/s in the presence and absence of inhibitors in natural seawater. In order to test the reproducibility of the results, the experiments were performed in triplicate.

2.3. Electrochemical Impedance Spectroscopy (EIS)

Electrochemical impedance measurements were conducted using a potentiostat/ galvanostat (Model PGSTAT 12, AUTOLAB, (ECO CHEMIE B.V Netherlands) the Netherlands B.V) with frequency response analyzer (FRA). The impedance measurements were carried out at an open circuit potential (OCP), after 30 min immersion of the brass electrode in the corrosive medium. The impedance data were acquired in the frequency range of 100 KHz–50 mHz with an AC voltage amplitude of 10 mV.

2.4. Analysis of FT-IR Spectroscopy

The film surface formed on the brass in the presence of the inhibitor was collected by scrapping from the surface of the alloy for spectral analysis with Fourier Transform Infrared spectroscopy (FT-IR). FT-IR spectra were recorded between 4000 cm^{-1} and 400 cm^{-1} using 12 scans with a resolution of 1 cm^{-1} using a Perkin-Elmer Model 577 spectrometer.

2.5. Inductively Coupled Plasma Atomic Emission Spectroscopy (ICP-AES)

The concentration of copper and zinc in the electrolytes, after the polarisation experiments in the presence and absence of 10^{-2} M thiadiazole derivatives, were determined by Inductively Coupled Plasma Atomic Emission Spectroscopy (ICPAES). An ICPAES (ARCOS from M/s. Spectro, Germany) was used to measure the amount of dissolution of zinc and copper from the brass surface. The dezincification factor (z) was calculated using the equation [14],

$$z \; = \; \frac{[C_{Zn}/C_{Cu}]_{sol}}{[C_{Zn}/C_{Cu}]_{alloy}} \tag{1}$$

where, $[C_{Zn}/C_{Cu}]_{sol}$ and $[C_{Zn}/C_{Cu}]_{alloy}$ are the ratios between the concentrations of zinc and copper in the solution and in the alloy respectively.

### 2.6. SEM and EDX investigations

The brass surface was prepared for SEM and EDX studies by keeping the specimens for an hour in the electrolyte with and without the optimum concentrations of the inhibitors. The brass specimens were then washed with distilled water dried and analyzed using SEM/EDX. A Philips

model XL30SFEG scanning electron microscope with an energy dispersive X-ray analyzer attached was used for surface analysis.
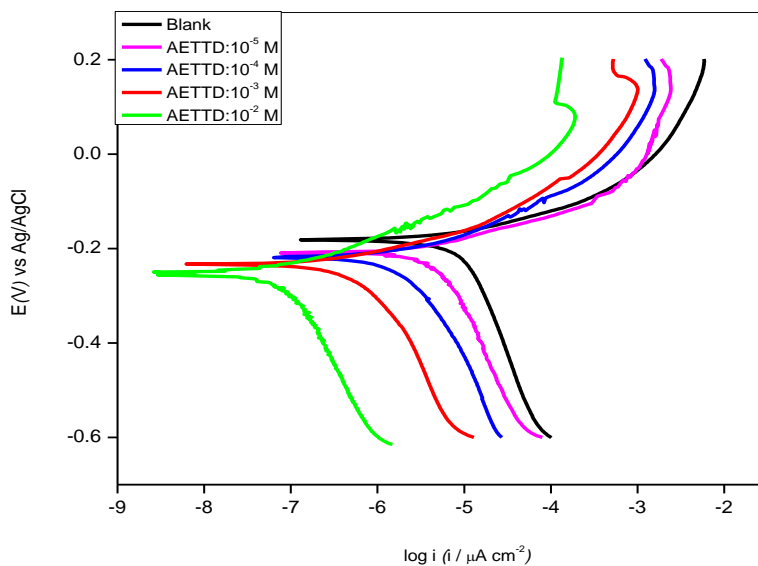
3. RESULTS AND DISCUSSION

3.1. Potentiodynamic polarisation studies

The anodic and cathodic polarisation curves of brass in natural seawater in the presence and absence of varying concentrations of AETD, AETTD and ATBTD are shown in Fig. 2(A-C).
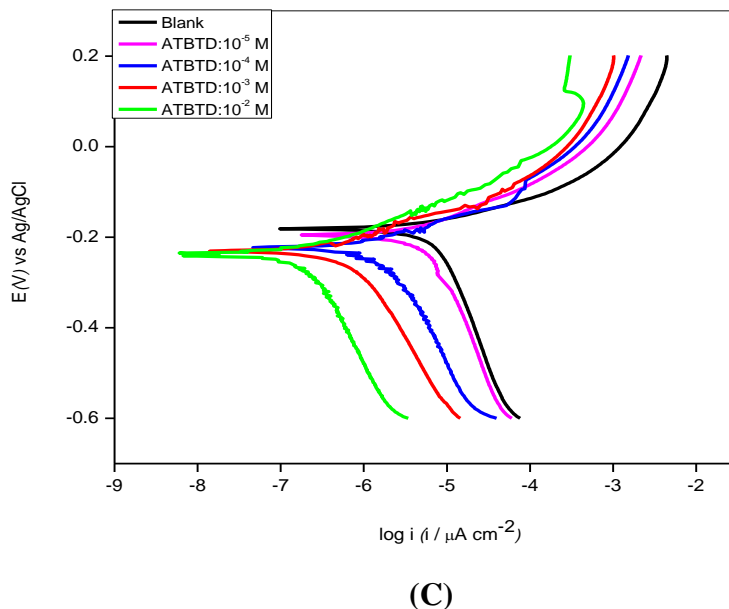

(A)

(B)

(C)
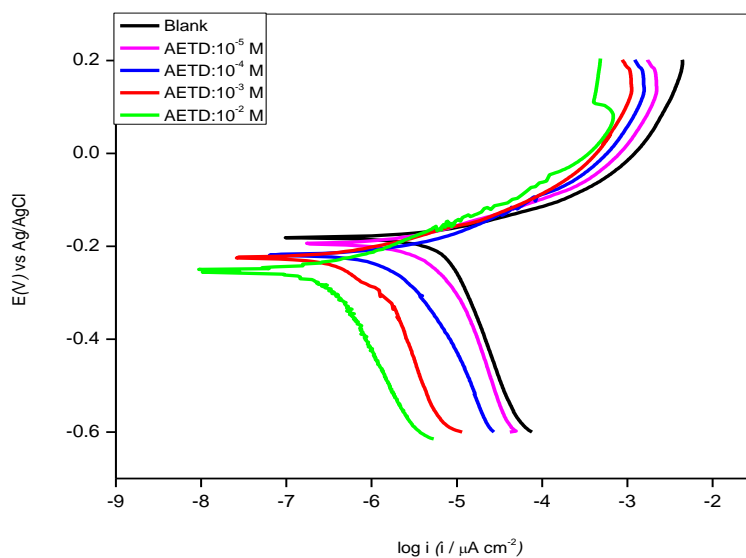
Figure 2. Potentiodynamic polarisation curves of brass in natural seawater in the absence and presence of different concentrations of AETD, AETTD and ATBTD.

The Tafel extrapolation method was used to calculate the corrosion parameters from the polarisation curves in the absence and the presence of different concentrations of inhibitors are given in Table 1. The inhibition efficiency (IE) was calculated using the equation:

$$IE\,(\%)\;\;=\;\frac{I_{corr} - I_{corr(inh)}}{I_{corr}} \times 100 \tag{2}$$

where, I_{corr} and $I_{corr(inh)}$ are the corrosion current densities without and with inhibitors, respectively. From the table, it is clear that the anodic and cathodic Tafel slopes are found to increase with increase in inhibitor concentration, which indicates that the inhibitors affect the kinetics of brass dissolution. Small changes in potentials are due to the result of the competition of the anodic and the cathodic inhibiting reactions, and of the brass surface condition. Thus these inhibitors act as mixed type inhibitors for brass in natural seawater. The inhibitors act as relatively mixed type for brass [15]. The increase in β_a and β_c are related to the decrease in both the anodic and cathodic currents. This indicates that the thiadiazole derivatives studied, inhibit the corrosion process of brass effectively and their ability as a corrosion inhibitor is enhanced as their concentration is increased.

The shift of E_{corr} values towards negative direction in the presence of thiadiazole derivatives, irrespective of their molecular structure or concentration in seawater, can be explained by the domination of cathodic reaction inhibition [16]. The change of potential in the negative direction can be attributed to the dissolution of native oxide and to the rapid formation of protective film on the brass surface, acting as barriers to the diffusion of oxygen molecules from the solution to the brass surface. However, it is clearly observed from the figures that the thiadiazole derivatives reduce both the anodic and cathodic current densities, indicating the inhibiting effect of the compounds.

Table 1. Potentiodynamic polarisation parameters for the corrosion of brass in natural seawater in the presence and absence of different concentrations of AETD, AETTD and ATBTD

.

| Compound	Concn (M)	$-E_{corr}$ (mV)	I_{corr} ($\mu A\ cm^{-2}$)	$-\beta_c$ mV/dec	β_a mV/dec	CR(mm.y^{-1}) $\times 10^{-3}$	IE (%)
Blank	-	181	2.65	34	40	110	-
AETD	10^{-5}	194	1.79	49	51	70	32
	10^{-4}	217	0.99	54	55	40	63
	10^{-3}	224	0.57	61	63	20	78
	10^{-2}	233	0.29	67	69	10	89
AETTD	10^{-5}	208	1.60	52	61	70	40
	10^{-4}	225	0.53	62	66	20	80
	10^{-3}	236	0.22	81	85	10	92
	10^{-2}	244	0.13	83	87	10	95
ATBTD	10^{-5}	198	1.75	52	62	70	34
	10^{-4}	223	0.97	58	64	40	63
	10^{-3}	230	0.55	67	74	20	79
	10^{-2}	235	0.24	78	82	10	91

The order of their inhibition efficiency is AETTD > ATBTD and > AETD.

*3.2. Electrochemical Impedance Spectroscopic measurements*

The impedance diagrams represented in Nyquist plot obtained at open-circuit potential after one hour immersion in seawater in the presence and absence of thiadiazole derivatives are presented in Fig. 3(A-C). The equivalent circuit in Fig.4 has been proposed for brass in seawater with thiadiazole derivatives [17-19].
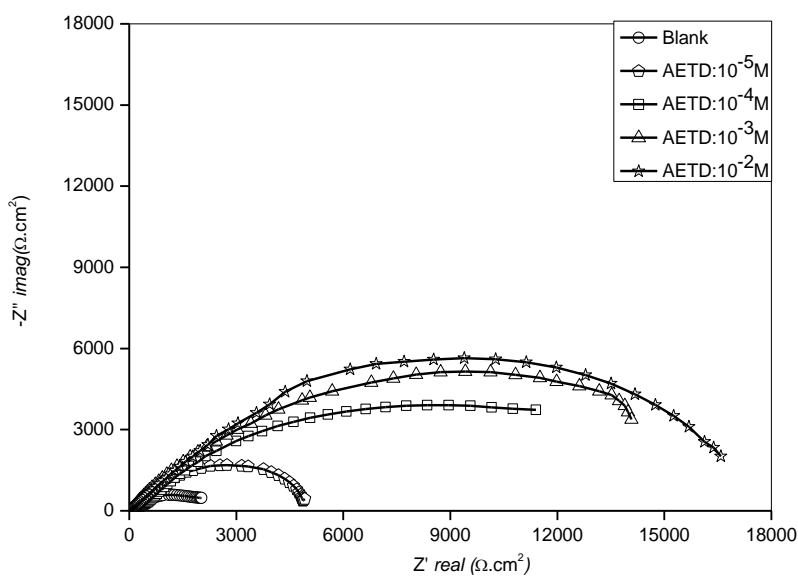
(A)
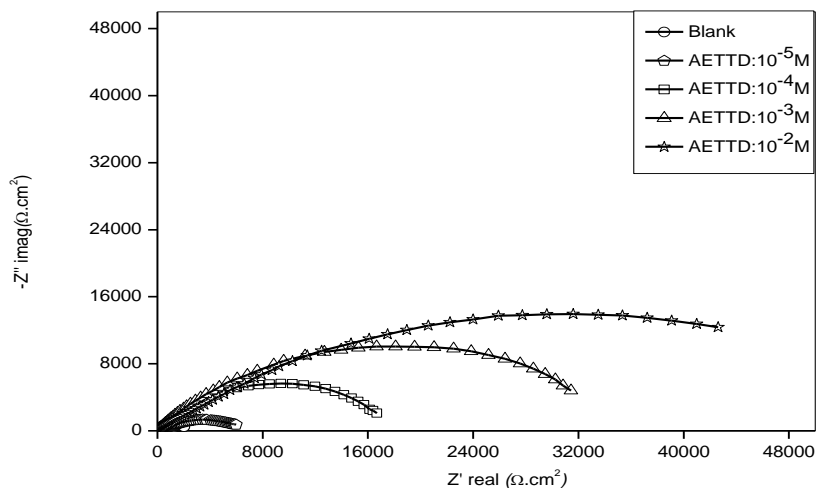
(B)
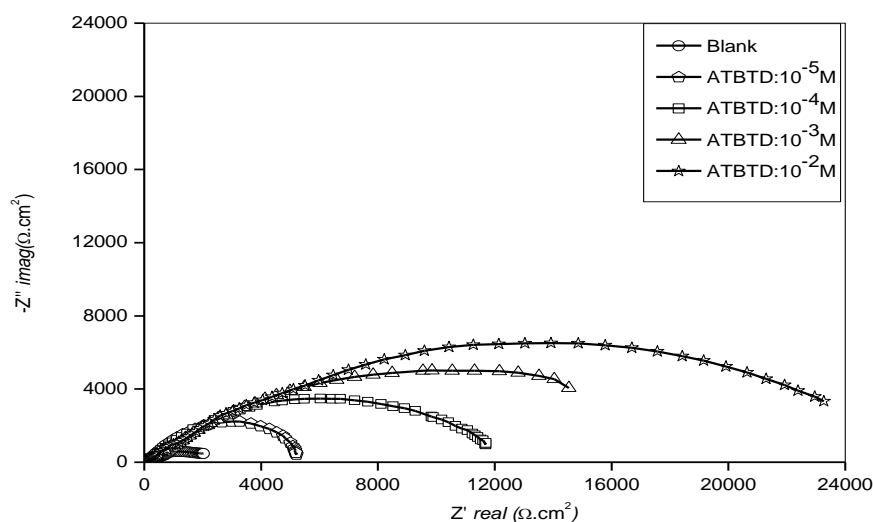
(C)

Figure 3. Nyquist plots of brass for brass in natural seawater in the absence and presence of different concentrations of AETD, AETTD and ATBTD.

The calculated parameters obtained from equivalent circuit fitting analysis with and without inhibitor in seawater are given in Table 2. In this calculation, instead of a pure capacitance, the distribution of the time constant for RC couple was used. A capacitive loop is calculated according to the following equation [20]

$$Z = \frac{R}{1+(j\omega RC)^n} \qquad \text{Where } 0 < n \leq 1$$

From this equation with distribution of time constant by n, C has the dimension of F/cm^2 and corresponds to the value at the frequency of the apex in Nyquist diagram.

Table 2. Electrochemical impedance parameters and inhibition efficiency for corrosion of brass in natural seawater in the presence and absence of different concentration of AETD, AETTD and ATBTD.

Inhibitor conc. (M)	R_s (Ω cm^2)	R_f (Ω cm^2)	C_f (μF cm^{-2})	n_f	R_{ct} (Ω cm^2)	C_{dl} (μF cm^{-2})	n_{dl}	R_F (Ω cm^2)	C_F (μF cm^{-2})	n_F	IE (%)
Blank	45	-	-	-	2750	165	0.68	3225	28	0.68	-
AETD											
10^{-5}	76	1010	43	0.79	3830	78	0.73	4020	15	0.74	33
10^{-4}	108	1375	33	0.80	6780	35	0.73	7985	13	0.75	63
10^{-3}	119	1796	24	0.80	12800	24	0.75	13510	10	0.76	79
10^{-2}	175	3225	12	0.83	25890	21	0.76	26150	9	0.81	89
AETTD											
10^{-5}	175	2010	9	0.90	3860	12	0.87	4060	8	0.88	40
10^{-4}	224	4690	6	0.91	12090	9	0.88	12780	6	0.89	80
10^{-3}	267	7570	4	0.91	29430	6	0.89	29990	3	0.89	91
10^{-2}	426	15250	1	0.92	48750	3	0.90	49970	1	0.91	95
ATBTD											
10^{-5}	89	1130	33	0.86	3840	46	0.80	4040	14	0.81	34
10^{-4}	124	1640	19	0.86	6810	33	0.81	8020	12	0.81	64
10^{-3}	169	2610	16	0.87	13020	22	0.81	13610	10	0.82	80
10^{-2}	219	4970	12	0.88	27820	19	0.82	28550	9	0.82	90

The use of this parameter, similar to the constant phase element (CPE), allowed the depressed feature of Nyquist plot to be reproduced readily.

It can be seen from the table that all three capacitances decrease with increase in concentration of inhibitors. The oxide film becomes slightly thicker (C_f), then the double layer capacitance (C_{dl}) decreases, and the amount available for the oxidation-reduction process (C_F) too decreases [21].
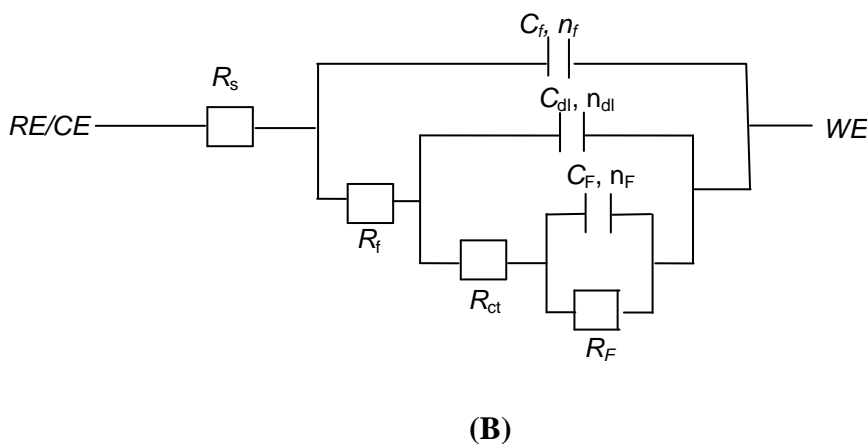

(A)

(B)
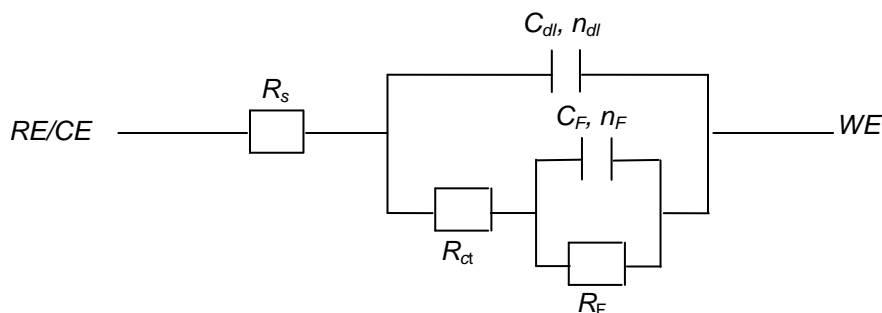
Figure 4. Equivalent electrical circuits of the experimental electrochemical impedance data (A) $R_s[C_{dl}$
$R_{ct}(C_F R_F)]$ and (B) $R_s\{ C_f R_f (C_{dl} R_{ct})[C_F R_F]\}$

The film resistance R_f increases with increase in the concentration of the thiadiazole derivatives, whereas the C_f values decreases proving that the surface film formed in presence of the investigated organic compounds is probably thicker, less permeable and highly adsorbed [22]. The charge transfer resistance (R_{ct}) increases and the double layer capacitance (C_{dl}) decreases on increase in concentration of the inhibitors indicating the decreased corrosion rate and increased corrosion inhibition, which is due to the adsorption of the inhibitor at the metal surface causing a change in the double layer structure. The decrease in C_{dl}, which results from local dielectric constant decrease and/or an increase in the thickness of the electrical double layer, suggests that these molecules act by adsorption on the metal/solution interface [23]. So, the changes in R_{ct} and C_{dl} values were caused by the gradual replacement of the water molecules by adsorption of inhibitor on brass surface, reducing the extent of dissolution [24]. The value of faradaic resistance (R_F) indicated the stability of surface film on the metal surface tends to increase with increase in concentration of the studied inhibitors. In the presence of inhibitors, the n_F values are found to be near 1, which shows that the films formed acts as an insulator. Therefore R_F is based on both the anodic process corresponding to the metal dissolution and/or the surface film formation, and the cathodic process.

The inhibition efficiency (IE) of the thiadiazole derivatives was calculated from the polarisation resistance values obtained from EIS measurements, according to the following equation:

$$IE\ (\%)\ =\ \frac{R_{p(inh)} - R_p}{R_{p(inh)}} \times 100 \qquad (4)$$

where, $R_{P(inh)}$ and R_P are polarisation resistance in the presence and absence of inhibitors in electrolytes respectively[25]. The inhibition efficiency increases with increase in concentration and maximum inhibition efficiency was obtained for AETTD. The % IE calculated from EIS shows the

same trend as those estimated from polarisation measurements i.e., polarisation measurements and EIS study complement each other well.

3.3. Adsorption Isotherm

The interaction of organic molecules with the metal during corrosion inhibition has been deduced in the form of adsorption characteristics of inhibitor. Inhibitors can function either by physical adsorption (electrostatic) or chemisorption on the metal surface. Different types of adsorption that take place involving organic molecules at the metal–solution interface are either: (a) the interaction of unshared pair of electrons in the inhibitor molecule with the metal surface, (b) the interaction of π-electrons of the inhibitor with the metal, (c) the electrostatic attraction between the charged inhibitor molecule and the charged metal or (d) the combination of all the three [26]. Different adsorption isotherms were analyzed in order to obtain more information about the interactions between thiadiazole derivatives and the brass surface. The linear relationship between θ values and C_{inh} are to be found in order to obtain the isotherm. The degree of surface coverage (θ) is calculated from the polarisation data using the following equations,

$$\theta \;=\; \frac{I_{corr} - I_{corr(inh)}}{I_{corr}}$$

(5)

where, I_{corr} and $I_{corr(inh)}$ are the corrosion current densities in the absence and in the presence of inhibitors, respectively.

Attempts were made to fit the θ values to various isotherms including Langmuir, Temkin, Frumkin and Flory-Huggins. The best fit is obtained with the Langmuir isotherm. The Langmuir adsorption isotherm is given by [27],

$$\frac{C_{inh}}{\theta} \;=\; C_{inh} + \frac{1}{K}$$

(6)

where, C_{inh} is the concentration of inhibitor, θ is the fractional surface coverage and K_{ads} is the adsorption equilibrium constant. A plot of C_{inh}/θ against C_{inh} shows a straight line indicating that adsorption follows the Langmuir adsorption isotherm [28] as shown in Fig. 5. The adsorption equilibrium constant, K obtained from the Langmuir adsorption isotherm is related to the standard free energy of adsorption (ΔG°_{ads}):

$$\Delta G^{\circ}_{ads} = -2.303RT\log(55.5K_{ads})$$

(7)

Where, R is the universal gas constant, T is the temperature and the value of 55.5 is the molar concentration of water in the solution [29]. The values of K_{ads} for AETD, AETTD and ATBTD are

809, 1808 and 1011 $dm^3.mol^{-1}$ respectively. The higher K_{ads} value (i.e., $\geq 100\ dm^3 mol^{-1}$), indicates that a stronger and more stable adsorbed layer has been formed, which increases the inhibition efficiency [30]. The higher value of K_{ads} for AETTD indicates stronger adsorption on the brass surface due to the presence of additional S donor atom than AETD and ATBTD.
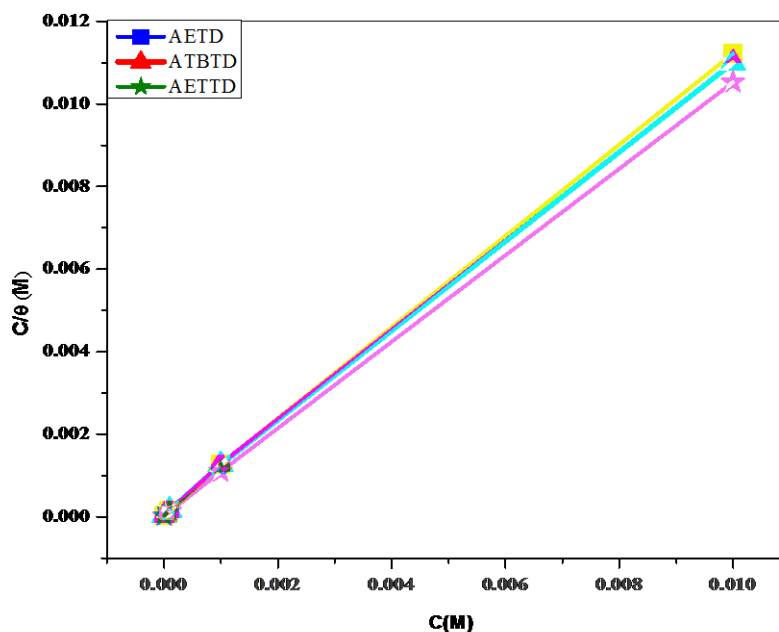

Figure 5. Langmuir adsorption isotherm plotted as(C/θ) versus C of AETD, ATBTD and AETTD in natural seawater.

ΔG°_{ads} values for AETD, AETTD and ATBTD are -27, -28 and -29 $kJ.mol^{-1}$ respectively. The negative ΔG°_{ads} values, calculated from the above equation is consistent with the condition for spontaneity of the adsorption process and the stability of the adsorbed layer on the brass surface. Generally, the enthalpy of adsorption values of -20 $kJ.mol^{-1}$ or lower are associated with an electrostatic interaction between charged molecules and charged metal surface, i.e., physisorption and values of -40 $kJmol^{-1}$ or higher involve charge sharing or a transfer from the inhibitor molecules to the metal surface to form a coordinate covalent bond, i.e., chemisorptions [31]. The values obtained for thiadiazole derivatives on brass in natural seawater lie in the range between -27 $kJ.mol^{-1}$ and -29 $kJ.mol^{-1}$. This indicates that the adsorption of the thiadiazole derivatives takes place through charge transfer from the unshared electron pairs in N and S of inhibitor molecules interacting with d-orbital of the Cu and Zn to provide a protective chemisorbed film.

3.4. FT-IR spectroscopy

The FT-IR spectra obtained for AETD, ATBTD, AETTD and the corresponding spectra before and after polarisation study are presented in Fig.6 (a-c). In the case of pure compounds, the bands at
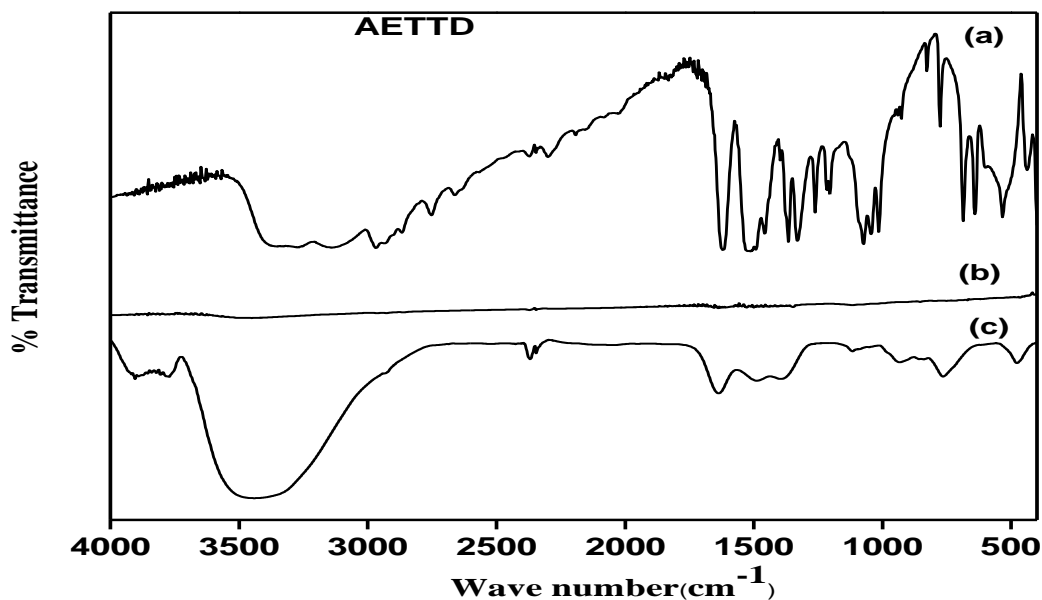
3289, 3116 cm^{-1} for AETD, 3354, 3141 for ATBTD and 3262, 3105 cm^{-1} for AETTD are assigned respectively to the asymmetrical and symmetrical N-H stretching vibrations of NH$_2$ group.   The symmetrical and asymmetrical C-H stretching vibrations due to the CH$_3$ and CH$_2$ groups of AETD, ATBTD and AETTD are observed between 2979 cm^{-1} and 2873 cm^{-1}.

(A)

(B)
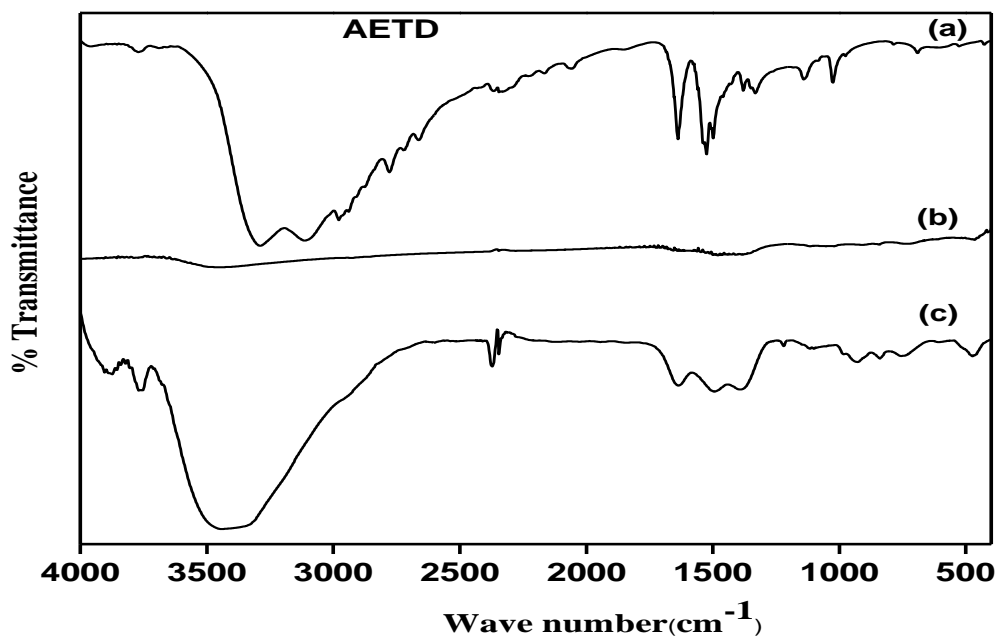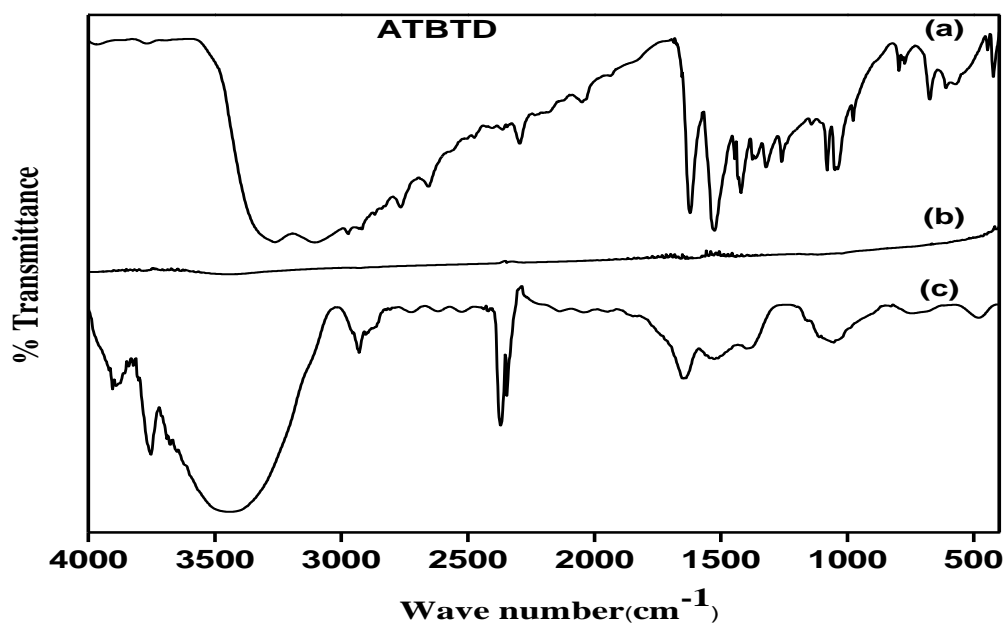
Figure 6. FT-IR spectra of (A) AETD, ATBTD and AETTD, (B) before polarisation and (C) after polarisation study of the inhibitor films formed on brass surface.

The strong peaks at 1628, 1621 and 1622 cm^{-1} are attributed to the (N H) in-plane bending vibrations of the amino group in AETD, ATBTD and AETTD respectively. For the three compounds the strong bands at 1525, 1514 and 1525 cm^{-1} are assigned to the stretching vibrations of the C=N group in the ring. The ring N-N stretching vibrations for the compounds AETD, ATBTD and AETTD are observed at 1026, 1045 and 1050 cm^{-1} respectively. The weak peaks at 774, 776 and 796 cm^{-1} are attributed to the N-H out of plane bending vibrations of the amino group in AETD, ATBTD and AETTD respectively. The ring C- S vibrations for AETD, ATBTD and AETTD are observed at 691, 687 and 675 cm^{-1} respectively. The strong peak at 1262 cm^{-1} for ATBTD is due the (CH$_3$)$_3$-C group. The strong peaks at 1260 and 1080 cm^{-1} for AETTD are attributed to the C-S stretching of the side chain. However, the peaks are very weak before polarisation study due to the chemisorptions of the inhibitors with the brass surface.

After polarisation, the peaks for the corresponding groups in AETD, ATBTD and AETTD vary after polarisation study due to the complex formation of inhibitors with metals. The N-H stretching vibration due to the surface films of all the three compounds derived from AETD, ATBTD and AETTD were shifted to higher frequency indicating the complex formation with metal involving the NH$_2$ group. The peaks for the surface films derived from AETD, ATBTD and AETTD due to N-H in-plane bending vibrations of the amino group are observed respectively at 1637, 1637 and 1648 cm^{-1}. The peaks assigned to the stretching vibrations of the C=N group in the ring for the corrosion products derived from AETD, ATBTD and AETTD are shifted to lower frequency and are observed at 1493, 1490 and 1516 cm^{-1} respectively. This indicates that there is coordination of the ring to the metal

surface. All the corrosion products derived from the adsorbed layer of AETD, ATBTD and AETTD show a strong peak at 1390 cm^{-1} due to the oxides of copper.

3.5. ICP-AES Analysis

The concentrations of copper and zinc in solutions containing 10^{-2} M of the thiadiazole derivatives after polarisation measurements were determined from inductively coupled plasma atomic emission spectroscopic (ICP-AES) analysis. The dezincification (z) factors for brass in the absence and presence of 10^{-3} M of AETD, AETTD and ATBTD in natural seawater were calculated from the ICP-AES data and the results are given in Table 3.

Table 3. Effect of AETD and AETTD and ATBTD on the dezincification of brass in natural seawater at optimum concentration (10^{-2} M)

Inhibitors	Solution analysis		Dezincification factor (z)	Percent inhibition	
	Cu/ 10^{-8} M	Zn/ 10^{-8} M		Cu (%)	Zn (%)
Blank	74	1725	43	-	-
AETD	11	194	33	85	89
AETTD	7	105	28	91	94
ATBTD	10	168	31	86	90

The results showed that both copper and zinc were present in the electrolyte in very small quantities and the copper to zinc ratio was found to be lesser than that of the bulk alloy. This is due to the surface barrier arising out of the growth of surface film of inhibitor on the metal surface as well as the corrosion product Cu_2O and ZnO. It is clear from the table that dezincification was much higher in the absence of inhibitors, while dezincification was much lower in the presence of 10^{-2} M concentration of AETD, AETTD and ATBTD. This indicated that the AETD, AETTD and ATBTD were able to minimize the dissolution of both zinc and copper. These values correlate with the corrosion rate and inhibition efficiency obtained by electrochemical methods.

3.6. SEM and EDX Analysis

Both SEM and EDX investigations were carried out to verify whether the studied inhibitors, AETD, ATBTD and AETTD are adsorbed on brass surface. The SEM micrograph for brass surface in the absence and presence of optimum concentration of thiadiazole derivatives are shown in Fig.7 (A-D). The micrographs of the surface after polarisation experiment are analyzed. The brass surface in the absence of inhibitors was found to be severely affected in seawater (Fig.7A). The metallic surface

seems to be not affected by corrosion in the presence of AETD, ATBTD and AETTD inhibitor molecules (Fig.7 B-D). At the optimum concentration of the inhibitors, the surface is covered by a thin film of inhibitor which effectively controls the dissolution of brass. A comparison of SEM micrographs obtained in the absence and in the presence of the AETD, ATBTD and AETTD molecules reveals a significant inhibiting effect of these compounds.
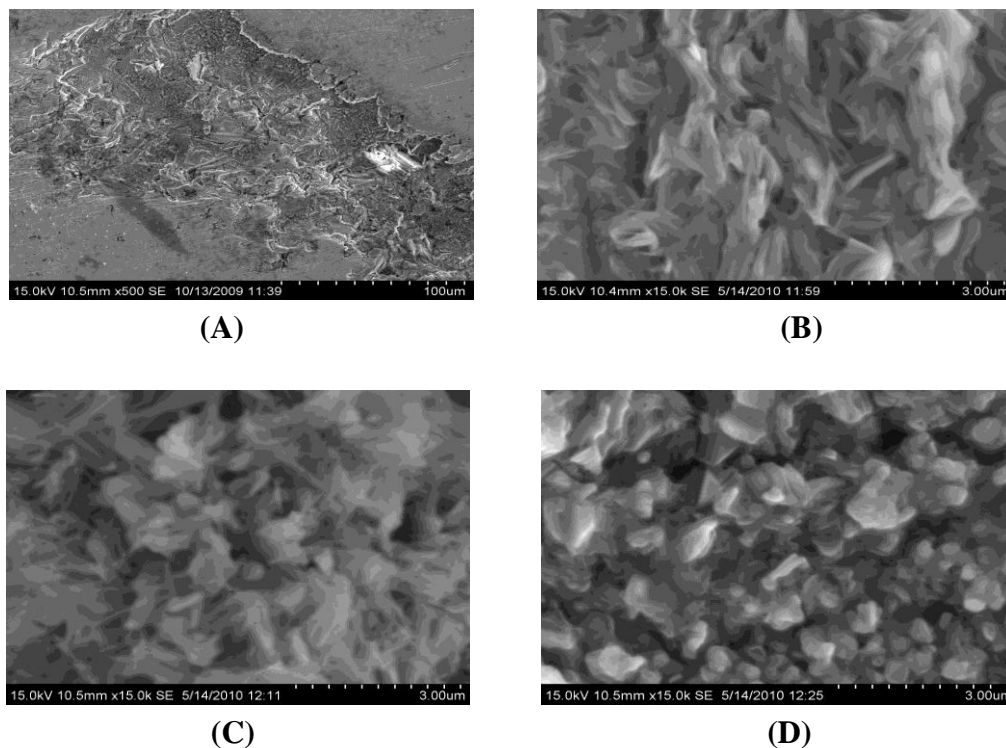

Figure 7. SEM images of brass (A) uninhibited surface (B-D) inhibited surface by AETD, ATBTD and AETTD

EDX spectroscopy was used to determine the elements present on the brass surface before and after exposure to the inhibitor solution. Fig.8 (A-D) presents the EDX spectra for the samples in the absence and presence of optimum concentrations of thiadiazole derivatives. In the absence of inhibitor molecules, the spectrum confirms the existence of chlorine and oxygen due to the formation of oxides and chlorides of both copper and zinc complexes. However, in the presence of the optimum concentrations of the inhibitors, AETD, ATBTD and AETTD, nitrogen and sulfur atoms are found to be present on the brass surface. This indicates that the inhibitor molecules are adsorbed on the brass surface and hence protect the brass surface against corrosion.

3.7. Mechanism of Corrosion Inhibition

The thiadiazole derivatives of the studied compounds contain polar groups such as sulfur and nitrogen. Each atom is a chemisorption centre and the inhibition efficiency depends on the electron

density around the chemisorption centre; higher the electron density at the chemisorption centre, greater is the inhibition efficiency.
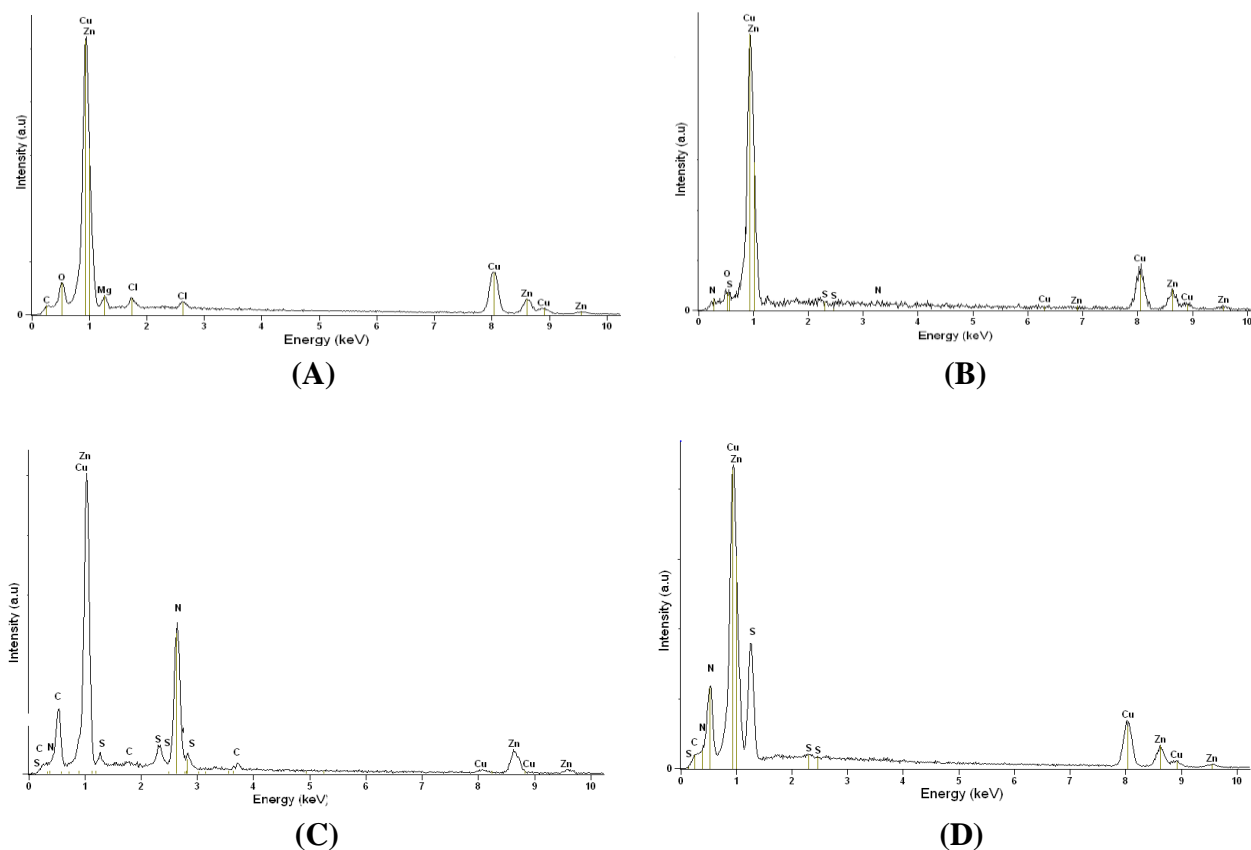

Figure 8. EDX profile for brass surface (A) blank, (B) AETD, (C) ATBTD and (D) AETTD.

The highest inhibition efficiency was observed for AETTD as it has an additional sulfur atom with lone pair of electrons. These electrons interact with the vacant d-orbital of copper present in the brass surface and adsorb strongly thereby blocking more number of adsorption sites on the brass surface [32]. When compared to AETD, ATBTD has better efficiency as its molecular size is more and the tertiary butyl group has higher electron donating property than the ethyl group. It has been previously reported in literature, that inhibiting effect depends mainly on inhibitor concentration, the molecular structure, size and structure of the side chain in the organic compounds [33]. It is observed that, the inhibition efficiency of the thiadiazole derivatives increases with increase in concentration as a result of higher surface coverage in solutions containing higher concentration of inhibitors.

4. CONCLUSIONS

Thiadiazole derivatives, namely, 2-amino-5-ethyl-1, 3, 4-thiadiazole (AETD), 2-amino-5-ethylthio-1, 3, 4-thiadiazole (AETTD) and 2-amino-5-tert-butyl-1, 3, 4-thiadiazole (ATBTD) have proved to be good inhibitors for the corrosion of brass in natural seawater. These inhibitors act as

mixed type inhibitors. IE % was found to increase with increase in concentration of inhibitors. The calculated from EIS show the same trend as those estimated from polarisation measurements. The inhibition of brass in natural seawater was found to obey Langmuir adsorption isotherm. The negative values of $\Delta G°_{ads}$ indicate spontaneous adsorption of the inhibitors on the surface of brass. Surface morphological studies such as FTIR, EDX and SEM analysis showed that a film of inhibitor is formed on the electrode surface. ICP-AES analysis revealed that the inhibitors effectively control the dezincification of brass.

References

1. Milan M. Antonijević, Snežana M. Milić, Marija B. Petrović, *Corros. Sci.*, 51 (2009) 1228
2. F. M. Kharafi, B. G. Ateya and R. M. Abd Allah, *J. Appl. Electrochem.*, 34 (2004) 47
3. M.M. Antonijevic, S.M. Milic, M.B. Radovanovic, M.B. Petrovic and A.T. Stamenkovic, *Int. J. Electrochem. Sci.*, 4 (2009) 1719
4. R. Ravichandran and N. Rajendran, *Appl. Surf. Sci.*, 239 (2005) 182
5. T. Murakava, S. Nagaura and N. Hackerman, *Corros. Sci.*, 7 (1967) 79
6. M. Abdallah, M. Al- Agez and A.S. Fouda, *Int. J. Electrochem. Sci.*, 4 (2009) 336
7. E. M. Sheriff and Su-Moon Park, *Electrochim. Acta*, 51 (2006) 6556
8. S. Mamas, T. Kiyak, M. Kabasakalogu and A. Koc, *Mater. Chem. Phys.*, 93 (2005) 41
9. S. Tamilselvi, V. Raman and N. Rajendran, *J. Appl. Electrochem.*, 33 (2003) 1175
10. M. M. Antonijevic, G. D. Bogdanovic, M. B. Radovanovic, M. B. Petrovic and A.T. Stamenkovic, *Int. J. Electrochem. Sci.*, 4 (2009) 654
11. F. Bentiss, M.Lebrini, H. Vezin, M.Lagrenee, *Mater. Chem. Phys.*, 87 (2004) 18
12. S.M. Milić, M.M. Antonijević, *Corros. Sci.*, 51 (2009) 28
13. R. Ravichandran, S. Nanjundan and N. Rajendran, *J. Appl. Electrochem.*, 34 (2004) 1171
14. R. Ravichandran, S. Nanjundan and N. Rajendran, *Appl. Surf. Sci.*, 236 (2004) 241
15. A.S. Fouda, H.A. Mostafa and H.M. El-Abbasy, *J. Appl. Electrochem.*, 40 (2010) 163
16. C. I. S. Santos, M. H. Mendonca and I. T. E. Fonseca, *J. Appl. Electrochem.*, 36 (2006) 1353
17. H. Otmacic Curkovic, E. Stupinisek-Lisac and H. Takenouti, *Corros. Sci.*, 51 (2009) 2342
18. M. Benmessaoud, K. Es-salah, N. Hajjaji, H.Takenouti, A. Shriri and M. Ebentouhami, *Corros. Sci.*, 49 (2007) 3880
19. H. Otmacic Curkovic, E. Stupinisek-Lisac and H. Takenouti, *Corros. Sci.*, 52 (2010) 398
20. L.Muresan, S.Varvara, E.Stupnisek-Lisac, H.Otmacic, K.Marusic, S.Horvat-Kurbegovic, L. Robbiola, K. Rahmounif and H. Takenouti, *Electrochim. Acta*, 52 (2007) 7770
21. K. Rahmouni, N. Hajjaji, M. Keddam, A. Srhiri, H. Takenouti, *Electrochim.Acta*, 52(2007)7519
22. K. Rahmouni, M. Keddam, A. Srhiri and H.Takenouti, *Corros. Sci.*, 47(2005) 3249
23. S. Muralidharan, K. L. N. Phani, S. Pitchumani and S. Ravichandran, *J. Electrochem. Soc.*, 142 (1995) 1478
24. B. Trachli, M. Keddam, H.Takenouti and A. Srhiri, *Corros .Sci.*, 44 (2002) 997
25. S. Varvara, L.M. Muresan, K. Rahmouni and H. Takenouti, *Corros. Sci.*, 50 (2008) 2596
26. D. Schweinsberg, G.George, A. Nanayakkara and D. Steiner, *Corros. Sci.*, 28 (1988) 33
27. M. Lebrini, F.Bentiss, H. Vezin and M. Lagrenee, *Corros. Sci.*, 48 (2006) 1279
28. E. Chaieb, A. Bouyanzer, B. Hammouti and M. Benkaddour, Appl. Surf.Sci., 246 (2005)199

29. O.Olivaries, N.V.Likhanova, B.Gomez, J.Navarrete, M.E.Llanos-Serrano, E.Arce and J.M.Hallen, *Appl. Surf. Sci*.,, 252 (2006) 2894
30. M. Lagrenee, B. Mernari, M. Bouanis, M. Traisnel and F. Bentiss, *Corros. Sci*., 44 (2002) 573
31. Simona Varvara, Liana Maria Muresan, Kamal Rahmouni and Hisasi Takenouti, *Corros. Sci*., 50 (2008) 2596
32. E.M. Sherif, *Appl. Surf. Sci*., 252 (2006) 8615
33. Kesenija Babic – Samardzija, Corina Lupu, Norman Hacherman, Andrew R. Barron and Andreas Luttge*, Langmuir*, 21(2005) 12187